

Lawrence Berkeley National Laboratory

Lawrence Berkeley National Laboratory

Title

Influence of the Torsion Angle in 3,3'-Dimethyl-2,2'-bipyridine on the Intermediate Valence of Yb in $(C_5Me_5)_2 Yb(3,3'-Me_2\text{-bipy})$

Permalink

<https://escholarship.org/uc/item/4pp7267x>

Author

Nocton, Grégory

Publication Date

2013-10-14

DOI

10.1021/om400528d

Peer reviewed

Influence of the Torsion Angle in 3,3'-Dimethyl-2,2'-bipyridine on the Intermediate Valence of Yb in $(C_5Me_5)_2Yb(3,3'-Me_2-bipy)$

Grégory Nocton,^{*†‡} Corwin H. Booth,[§] Laurent Maron,[⊥] and Richard A. Andersen^{*‡§}

[†]Laboratoire Hétéroéléments et Coordination, CNRS, Ecole Polytechnique, Palaiseau, France.

[‡]Department of Chemistry, University of California Berkeley, Berkeley, California, 94720, USA.

[§]Chemical Science Division, Lawrence Berkeley National Laboratory, Berkeley, California, 94720, USA.

[⊥]LPCNO, UMR 5215, Université de Toulouse-CNRS, INSA, UPS, Toulouse, France.

Abstract.

The synthesis and X-ray crystal structures of $Cp^*_2Yb(3,3'-Me_2bipy)$ and $[Cp^*_2Yb(3,3'-Me_2bipy)][Cp^*_2YbCl_{1.6}I_{0.4}] \cdot CH_2Cl_2$ are described. In both complexes, the NCCN torsion angles are approximately 40° . The temperature independent value of n_f of 0.17 shows that the valence of ytterbium in the neutral adduct is multiconfigurational, in reasonable agreement with a CASSCF calculation that yields a n_f value of 0.27; that is, the two configurations in the wave function are $f^{13}(\pi^*_1)^1$ and $f^{14}(\pi^*_1)^0$ in a ratio of 0.27 to 0.73, respectively, and the open-shell singlet lies 0.28 eV below the triplet state (n_f accounts for f-hole occupancy, that is $n_f = 1$ when the configuration is f^{13} and $n_f = 0$ when the configuration is f^{14}). A correlation is outlined between the value of n_f and the individual ytterbocene and bipyridine fragments such that, as the reduction potential of the ytterbocene cation and the free x,x'-R₂-bipy ligands approach each other, the value of n_f and therefore the $f^{13}:f^{14}$ ratio reaches a maximum; conversely, the ratio is minimized as the disparity increases.

Introduction.

Previous studies of the 2,2'-bipyridine adduct of $(C_5Me_5)_2Yb$, abbreviated $Cp^*_2Yb(bipy)$ have shown that the electronic ground state is multiconfigurational; that is, the f-orbital portion of the ground state wave function includes $\Psi = c_1|Yb(III, f^{13})(bipy^{\cdot-}) \rangle + c_2|Yb(II, f^{14})(bipy)^0 \rangle$,

which is an admixture of two configurations, where c_1 and c_2 are their respective coefficients.¹ The $f^{13}(\text{bipy}^{\bullet})$ configuration is an open-shell singlet and $f^{14}(\text{bipy})^0$ is a closed-shell singlet and a configuration interaction is therefore possible since the two configurations have the same symmetry. The outcome of the configuration interaction is that the valence of the ytterbium in $\text{Cp}^*_2\text{Yb}(\text{bipy})$ is neither +II, where $c_1 = 0$, nor +III, where $c_2 = 0$, but is in between these two extreme values and therefore intermediate valent. Experimentally, the valence of the ytterbium was obtained from Yb L_{III}-edge XANES spectroscopy and expressed as n_f , the number of f- holes: for $\text{Cp}^*_2\text{Yb}(\text{bipy})$, $n_f = c_1^2 = 0.83(2)$, is temperature independent, and therefore $f^{13}(\text{bipy}^{\bullet})$ is the dominant configuration. The concept that the ground state is multiconfigurational, initially posited by Fulde,² was developed from CASSCF calculations, initially using the model $(\text{C}_5\text{H}_5)_2\text{Yb}(\text{bipy})$,¹ then extended to $(\text{C}_5\text{Me}_5)_2\text{Yb}(\text{bipy})$ and including four empty bipy orbitals, π^*_1 , π^*_2 , π^*_3 , and π^*_4 , in the active space. The calculated value of n_f was 0.86 in agreement with experiment.³

When the 2,2'-bipyridine ligand in $\text{Cp}^*_2\text{Yb}(\text{bipy})$ is replaced by methyl-substituted 2,2'-bipyridine ligands symbolized as x-Mebipy or x,x'-Me₂bipy where x indicates the position of the methyl group(s) in the 2-pyridyl rings, the ytterbium atom in the resulting adducts is intermediate valent, but the value of n_f is temperature dependent.³ For example when x is 5, the value of n_f in $\text{Cp}^*_2\text{Yb}(5\text{-Mebipy})$ changes from 0.42 to 0.75 at 300 K and 30 K, respectively. The temperature dependence is not due to a closed-shell singlet \rightleftharpoons open-shell triplet equilibrium, a valence tautomerism, but an equilibrium between two open-shell singlet states in which the thermodynamic constants, ΔH and ΔS are obtained using the Boltzmann equation. The computational model showed that two open-shell singlet states, SS1 and SS2, lie below the triplet by 0.58 eV and 0.11 eV, respectively.

The evolving model of the electronic structure of the bipyridine adducts of Cp^*_2Yb is, (i) the ground state is an open-shell singlet, (ii) the configurations of both fragments, Cp^*_2Yb and

the bipyridines are multiconfigurational, (iii) the number and position of the methyl groups on the bipyridine ligand, and (iv) the n_f values qualitatively track the reduction potential of the free bipyridine ligand, at least for those bipyridines whose reduction potentials are available in the literature. Item (iv) provides a strategy for manipulating the value of n_f and therefore the magnetic properties of the adducts. The reduction potential of a ligand is a measure of the HOMO-LUMO energy gap,^{1,2} which can be changed by substituents that are electron-donors or electron-acceptors and by the torsion angle between the 2-pyridyl rings, usually reported as the NCCN angle, obtained from solid-state crystal structures. Electron-donating groups, such as a methyl group, increase the reduction potential relative to hydrogen, Table 1, while a CO₂Me group decreases the potential. Increasing the torsion angle should raise the reduction potential, since twisting the 2-pyridyl groups out of coplanarity will move the energy of π^*_1 closer to the energy of π^*_2 and π^*_3 orbitals. Although the value of the reduction potential for 3,3'-Me₂bipy is not available in the literature, the energy of the empty orbital should behave qualitatively like those in twisted ethylene.⁴ Several examples of methyl- and dimethyl-substituted bipyridine adducts of Cp*₂Yb have been reported that are consistent with the correlation between n_f and the reduction potential. In this article, we prepared the neutral and cationic adducts between 3,3'-Me₂bipy and Cp*₂Yb in order to explore the physical properties of the adducts with a bipyridine ligand with a large torsion angle. The results of these and earlier studies support the contention that the redox properties of the individual molecular fragments that comprise the adduct, Cp*₂Yb and x,x'-Me₂bipy, determine the extent of electron correlation between them.

Table 1. Redox potential of selected N-aromatic heterocycles and ytterbocenes.

Ligand	$E_{1/2}$ (V) vs. Fc^+/Fc	Ref
py	-3.16	5
4,4'-(OEt) ₂ bipy	-2.88	6
4,4'-Me ₂ bipy	-2.68	6
bipy ^a	-2.60	7
4,4'-CO ₂ Me	-2.03	6
(C ₅ Me ₅) ₂ Yb ⁺	-1.78	8
(C ₅ H ₄ Me) ₂ Yb ⁺	-1.65	9

a) The approximate value of 3,3'-Me₂bipy lies below -2.8 V (vs. Fc^+/Fc , THF / 0.1 M [NBu₄][PF₆]) but could not be measured precisely under our conditions. Under similar conditions the value of bipy is 2.63 V (vs. Fc^+/Fc).

Results.

Synthesis and Physical Properties.

The preparation of Cp*₂Yb(3,3'-Me₂bipy) follows the general synthesis procedure used in earlier articles, that is, addition of 3,3'-Me₂bipy to Cp*₂Yb(OEt)₂¹⁰ in toluene followed by crystallization at -20°C. The green crystals melt at 310-312°C (Scheme 1).

Scheme 1.

The cation, [Cp*₂Yb(3,3'-Me₂bipy)][Cp*₂YbI₂] is obtained by addition of the neutral adduct to a suspension of AgI in toluene (Scheme 2). In this case, the identity of the anion depends upon crystallization solvent.^{11,12} If the cation-anion pair is crystallized from warm toluene, the ion-pair crystallizes as [Cp*₂Yb(3,3'-Me₂bipy)][Cp*₂YbI₂]·1/3PhMe. If, on the other hand,

the ion-pair is crystallized by layering a CH₂Cl₂ solution with pentane, the ion-pair has the composition [Cp*₂Yb(3,3'-Me₂bipy)][Cp*₂YbCl_{1.5}I_{0.5}]·CH₂Cl₂, as determined by combustion analysis and integrated intensities in the ¹H NMR spectrum, see Experimental Section for details. Although the composition of a single crystal is slightly different, [Cp*₂Yb(3,3'-Me₂bipy)][Cp*₂YbCl_{1.6}I_{0.4}]·CH₂Cl₂, see below, it is clear that chloride for iodide exchange occurs in dichloromethane, a result not observed in earlier studies of ytterbocenebipyridine cations.^{11,12}

Scheme 2.

X-ray Crystal Structures.

The ORTEP's of the neutral and cation adducts are shown in Figures 1 and 2. The crystallographic details are available in Supporting Information and some bond length and angles are listed in Table 2. In both adducts, the coordination number and geometry about ytterbium are the same as are the torsion angles in the coordinated 3,3'-Me₂bipy ligands, the intramolecular bond angles, and the C(2)-C(2') distances; the average Yb-N and Yb-C, however, are rather different. The average Yb-C distance in the neutral adduct of 2.71 ± 0.01 Å is the same as found in Cp*₂Yb(py)₂ of 2.74 ± 0.04 Å¹³ and in the three independent molecules of Cp*₂Yb(6,6'-Me₂bipy) of 2.74 ± 0.002 Å.³ However, the average Yb-N distance of 2.485 ± 0.003 Å is significantly shorter than the equivalent distances in Cp*₂Yb(py)₂ and Cp*₂Yb(6,6'-Me₂bipy) of 2.565 ± 0.005 Å and 2.506 ± 0.009 Å, respectively. The average Yb-C distance in the cation of 2.60 ± 0.01 Å is identical to that in

$[\text{Cp}^*_2\text{Yb}(\text{bipy})]^+$ of $2.59 \pm 0.01 \text{ \AA}$ as are the Yb-N distances of $2.396 \pm 0.02 \text{ \AA}$ and $2.372 \pm 0.005 \text{ \AA}$, respectively. The Yb-C and Yb-N distances in the neutral adduct are approximately 0.10 \AA longer than in the cation, showing that the valences of Yb are different.

It is noteworthy that the torsion angles of approximately 40° , defined by either the four atoms, NCCN, CCCC, or the dihedral angle between the planar 3-Me-2-pyridyl rings are the same in both adducts. The large torsion angle in $[\text{Cp}^*_2\text{Yb}(3,3'\text{-Me}_2\text{bipy})]^+$ of 40° and the small one in $[\text{Cp}^*_2\text{Yb}(\text{bipy})]^+$ of 7° results in only a slight elongation of the Yb-N distance (0.012 \AA) in the former. Hence, the large torsion angle and the resulting "misdirection" of the lone pair of electrons on the bidentate chelate in these cations only lengthens slightly the average Yb-N distances. This, presumably, reflects the small effect on the bond enthalpy difference resulting from the "misdirection". Several crystal structures of 3,3'-Me₂bipy with d-transition metals are known and the twist angle, generally defined as the intersection of the dihedral angle between the planar 3-Me-2-pyridyl rings range from 29° to 37° .¹⁴⁻²⁰ One exception is $[\text{Ru}(\text{Me}_3\text{tacn})(3,3'\text{-Me}_2\text{bipy})(\text{OH}_2)]^{2+}$, in which the reported twist angle is 54° . However, the structure in the CCDC, indicates that the NCCN and CCCC angles are 29° and 43° , respectively.¹⁷

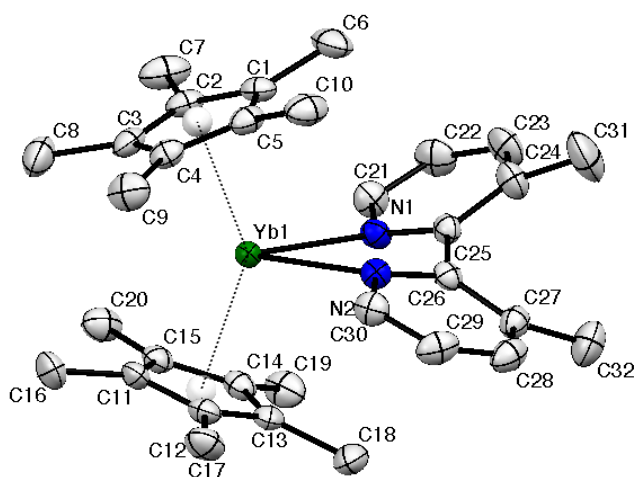


Figure 1. ORTEP of $\text{Cp}^*_2\text{Yb}(3,3'\text{-Me}_2\text{bipy})$ (thermal ellipsoids at 50% level). All non-hydrogen atoms are refined anisotropically and the hydrogen atoms are placed in calculated positions but not refined.

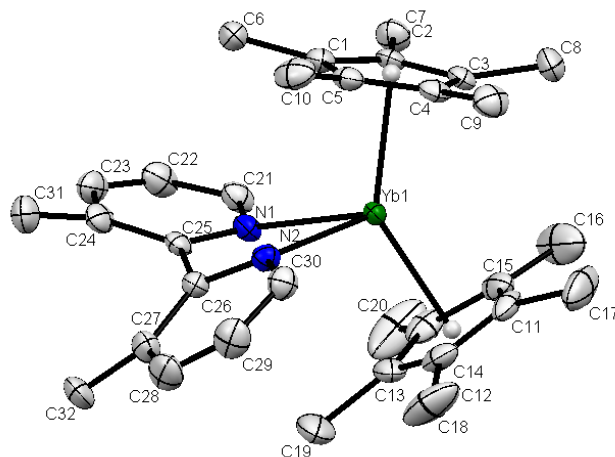


Figure 2. ORTEP of the cation $[\text{Cp}^*_2\text{Yb}(3,3'\text{-Me}_2\text{bipy})]^+$ (thermal ellipsoids at 50% level). The anionic partner $[\text{Cp}^*_2\text{YbCl}_{1.6}\text{I}_{0.4}]^-$ and the co-crystallized molecule of CH_2Cl_2 are removed for clarity. All non-hydrogen atoms are refined anisotropically and the hydrogen atoms are placed in calculated positions but not refined.

Table 2. Comparison of bond length (Å) and angles (deg) for $\text{Cp}^*_2\text{Yb}(3,3'\text{-Me}_2\text{bipy})$ and $[\text{Cp}^*_2\text{Yb}(3,3'\text{-Me}_2\text{bipy})]^+$.

	$\text{Cp}^*_2\text{Yb}(3,3'\text{-Me}_2\text{bipy})$	$[\text{Cp}^*_2\text{Yb}(3,3'\text{-Me}_2\text{bipy})]^+$	Δ^a
Yb-C(ring) (average)	2.71±0.01	2.60±0.01	0.11
Yb-C(ring) (range)	2.693(3) – 2.732(3)	2.585(4) – 2.629(4)	-
Yb-Cp(cent)	2.43	2.31	0.12
Yb-N(average)	2.485±0.003	2.393±0.002	0.09
C(25)-C(26)	1.494(5)	1.491(6)	0.003
Cp(cent)-Yb-Cp(cent)	147	141	6
Cp(cent)-Yb-N	103, 107	105, 108	2, 1
N-Yb-N	66.6(1)	69.6(1)	-3
N-C-C-N	38	37	1
C-C-C-C	44	43	1
3-Me-2-pyridyl	41	41	0

a) Δ is the value in the neutral adduct minus that in the cation in Å or deg.

¹H NMR Studies.

The ^1H NMR chemical shifts at 20°C of the previously prepared bipyridine and substituted bipyridine adducts of Cp^*_2Yb fall into a pattern in which δ 6-H (~ 160 ppm) $>$ δ 4-H (~ 30 ppm) $>$ δ 5-H (~ 10 ppm) $>$ δ 3-H (~ -15 ppm). The assignments are determined by H for Me group replacement; the approximate value of the chemical shifts are in parenthesis.²¹ The ^1H NMR spectra show that the adducts have C_{2v} symmetry in solution. The chemical shifts of the 3,3'- Me_2bipy adduct also show four bipy resonances at 20°C with δ_{H} values of 32.7, 12.1, 8.5, and 0.58 ppm. The only resonance that can be assigned with certainty is $\delta_{\text{H}} = 0.58$ due to the methyl groups in the 3,3' positions; the $\delta_{\text{H}} = 12.1$ resonances is a doublet and therefore is likely due to δ 4-H. The relatively small spread in chemical shift values relative to the large spread in the previously reported adducts of $\text{Cp}^*_2\text{Yb}(\text{x},\text{x}'\text{-bipy})$ where $\text{x} = \text{H}$ and $\text{x}' = \text{Me}$ or $\text{x} = \text{x}' = \text{Me}$, implies that the extent of paramagnetism is less in the 3,3'- Me_2bipy adduct. The small range in chemical shift values of the bipy resonances in $\text{Cp}_2\text{Yb}(\text{bipy})$ of δ_{H} 53, 18, 11 and 0.6 ²² implies that the two adducts have a similar degree of paramagnetism, an inference that is developed below.

A plot of δ vs. $1/T$ (Figure 3) of $\text{Cp}^*_2\text{Yb}(3,3'\text{-Me}_2\text{bipy})$ shows that the most downfield resonance has a strong dependence on temperature and the shift increases with increasing temperature, *i.e.*, the resonance shows anti-Curie behavior. A resonance that follows a Curie Law, $\delta = C/T$, has a positive slope in a δ vs. $1/T$ plot, but a slope that is negative displays anti-Curie behavior. This anti-Curie dependence is not due to the exchange between free and coordinated 3,3'- Me_2bipy since addition of 3,3'- Me_2bipy results in a spectrum at 20°C due to free and coordinated 3,3'- Me_2bipy resonances. Unfortunately, the inverse temperature dependence of the downfield resonance cannot be interpreted since the resonance cannot be assigned definitively although it is most reasonably ascribed to the 6-H position and therefore the value of its chemical shift is dominated by the dipolar contribution to the chemical

shift.¹² It is noteworthy that anti-Curie behavior has been shown in low spin Fe(III) porphyrins to result from a difference in sign between the dipolar and contact shift terms in the chemical shift tensor.²³

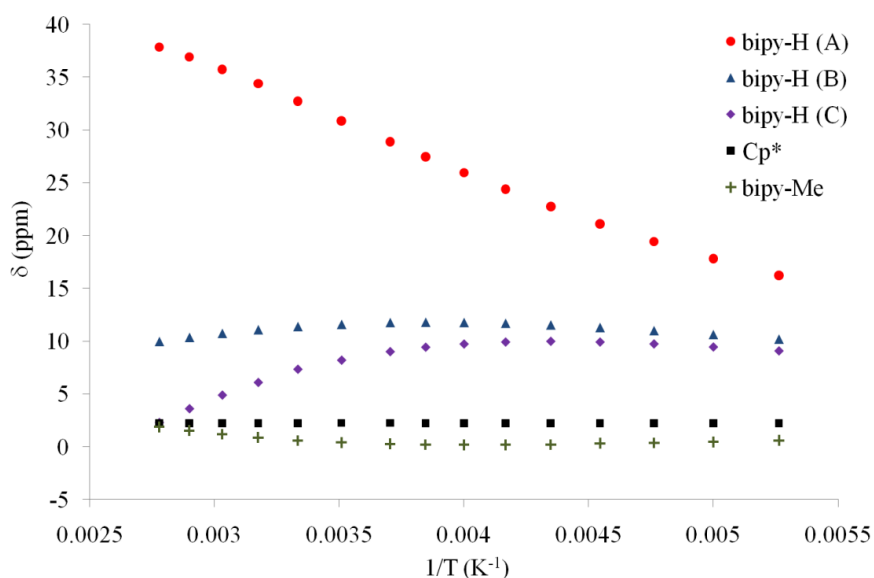


Figure 3. Chemical shift (δ) vs. $1/T$ plot of the proton resonances of $\text{Cp}^*_2\text{Yb}(3,3'\text{-Me}_2\text{bipy})$ in toluene- d_8 over a temperature range of 180K to 360K.

The symmetry of the neutral and cationic adducts of 3,3'- Me_2bipy have C_2 symmetry in the solid state (Figure 2 and 3). The ^1H NMR spectrum of the cation in CD_2Cl_2 at 300K contains four bipyridine resonances at 313, 52, 11 and -18 ppm; the intensity of the latter resonance shows that it is due to the methyl groups. Unfortunately, the resonance at $\delta_{\text{H}} = 313$ ppm disappears into the base-line as the temperature is lowered and its temperature dependence cannot be determined. In solution, the adducts could have either C_2 or C_{2v} symmetry depending on the value of the torsion angle. In C_{2v} symmetry the average torsion angle is zero and therefore the methyl groups on each 2-pyridyl ring are eclipsed. Thus the dynamic process of $C_2 \rightleftharpoons C_{2v} \rightleftharpoons C_2$ will have a high activation energy.²⁴⁻²⁷ This process cannot be observed in the $[\text{Cp}^*_2\text{Yb}(3,3'\text{-Me}_2\text{bipy})]^{0,+}$, since the two methyl groups are chemically equivalent in

either C_2 or C_{2v} symmetry. A way to answer this question would be to prepare adducts in which the C_2 -axis is removed, for example by preparing $CpCp'Yb(3,3'-Me_2bipy)$. Unfortunately, a synthetic methodology for preparing mixed-ring ytterbocenes is unknown at the present time.

Visible Spectroscopy.

Room temperature Vis-NIR spectra for $Cp^*_2Yb(3,3'-Me_2bipy)$ and $[Cp^*_2Yb(3,3'-Me_2bipy)][Cp^*_2YbCl_{1.5}I_{0.5}]$, recorded in toluene and CH_2Cl_2 , respectively, are shown in Figure 4. Two main bands at around 500 nm (20000 cm^{-1}) and 900 nm (11110 cm^{-1}) are present in $Cp^*_2Yb(3,3'-Me_2bipy)$. These two transitions, attributed to ligand based $\pi \rightarrow \pi^*$ and $\pi^* \rightarrow \pi^*$, are present as principal features in the spectrum of $Li(bipy)^{28}$ and are reasonably ascribed to radical anion signatures in this ytterbocene adduct. If correct, the absorption coefficients are low implying a low concentration of $3,3'-Me_2bipy$ radical anion. The intensity of the ligand based $\pi^* \rightarrow \pi^*$ transitions and the relatively small spread of the 1H NMR chemical shifts imply that the extent of the paramagnetism of $Cp^*_2Yb(3,3'-Me_2bipy)$ is small, which in turn implies that the f^{14} configuration dominates the $f^{13}(bipy^{\cdot-})$ configuration in the ground state electronic structure.

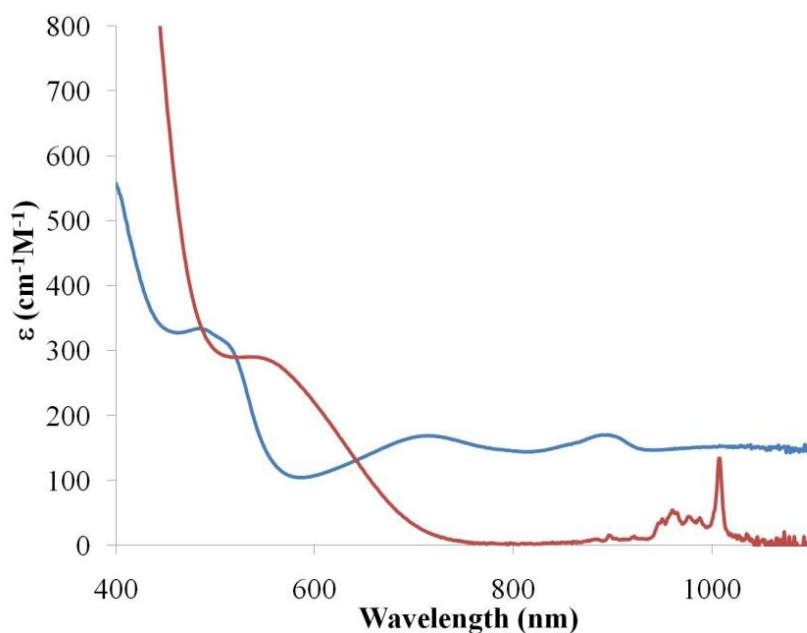


Figure 4. Room Temperature Visible Spectra of $\text{Cp}^*_2\text{Yb}(3,3'\text{-Me}_2\text{bipy})$ (blue line) in toluene and $[\text{Cp}^*_2\text{Yb}(3,3'\text{-Me}_2\text{bipy})][\text{Cp}^*_2\text{YbCl}_{1.5}\text{I}_{0.5}]$ (red line) in CH_2Cl_2 .

The cation, $[\text{Cp}^*_2\text{Yb}(3,3'\text{-Me}_2\text{bipy})][\text{Cp}^*_2\text{YbCl}_{1.5}\text{I}_{0.5}]$, possesses a simpler visible spectrum at room temperature and is similar to the reported spectra of cationic Cp^*_2Yb adducts with N-aromatic heterocycles.^{11,28} The presence of several f-f transitions in the 950-1020 nm range accounts for the multiple coordination environments of the anionic partner in the anion-pair.

Magnetism and XANES Studies.

The effective magnetic moment at 300 K for $\text{Cp}^*_2\text{Yb}(3,3'\text{-Me}_2\text{bipy})$ is $0.8 \mu_{\text{B}}$, low relative to the value expected for two uncorrelated spin carriers, $\text{Yb}(\text{III})$, f^{13} and bipy^- , for which the value of $4.85 \mu_{\text{B}}$ is expected. The low value of μ_{eff} is an indication that the Yb in the neutral adduct may be intermediate valent and therefore a member of the family of the bipyridine adducts of Cp^*_2Yb reported earlier in which effective moments range from $2.4 \mu_{\text{B}}$ to $0.8 \mu_{\text{B}}$ at 300 K. The temperature dependence of μ_{eff} from 2 K to 300 K is shown in Figure 5 (Plots of χ , $1/\chi$ and χT vs. T are available in SI).

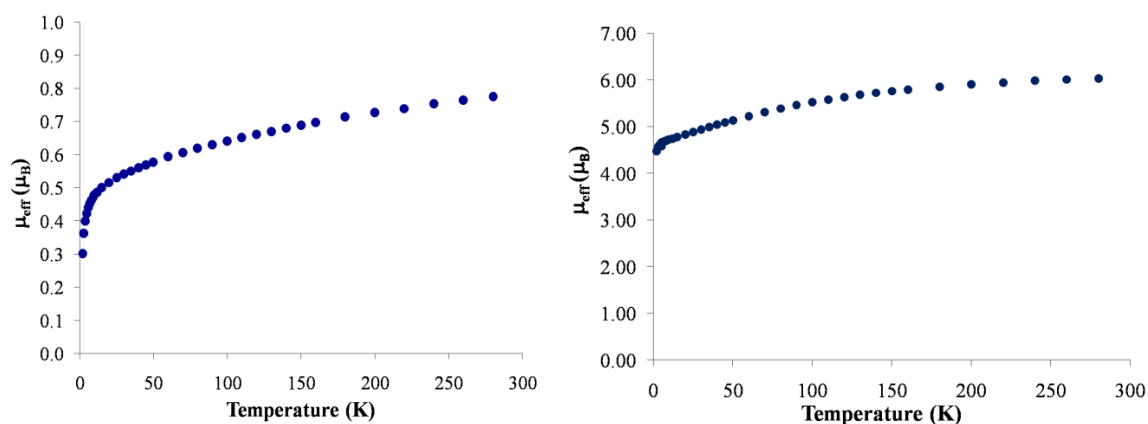


Figure 5. Temperature dependent magnetic susceptibility data for the neutral (left) and cationic ytterbocenes (right) between 2 K and 300 K.

The value of μ_{eff} decreases slowly in the neutral adduct with decreasing temperature to a value of $0.6 \mu_{\text{B}}$ at 30 K and then rapidly decreases to $0.3 \mu_{\text{B}}$ at 2 K. The latter decrease is likely due to intermolecular antiferromagnetic coupling at low temperature as previously observed.¹ In contrast, and as expected, the value of μ_{eff} for $[\text{Cp}^*_2\text{Yb}(3,3'\text{-Me}_2\text{bipy})][\text{Cp}^*_2\text{YbI}_2]$ of $6.1 \mu_{\text{B}}$ is in accord with the value for two Yb(III), $^2J_{7/2}$, isolated paramagnets of $6.4 \mu_{\text{B}}$. Although the low effective moment for the neutral adduct is a signature of intermediate valent ytterbium, a spectroscopic measurement is necessary to confirm this hypothesis. The Yb L_{III} -edge XANES^{1,3} spectra in Figure 6 shows that the Yb L_{III} -edge XANES at 30 K and 300 K are nearly superimposable and therefore the ratio of Yb(II), f^{14} to Yb(III), f^{13} is independent of temperature and rules out a valence tautomeric equilibrium as a possible explanation for the temperature dependence of μ_{eff} . The XANES spectra can be fit into f^{14} and f^{13} components in a ratio of 83:17 at both temperatures and the resulting n_{f} value is therefore 0.17. These results place $\text{Cp}^*_2\text{Yb}(3,3'\text{-Me}_2\text{bipy})$ into a small subset of bipyridine adducts with low values of μ_{eff} and n_{f} at 300 K reported previously (Table 3).

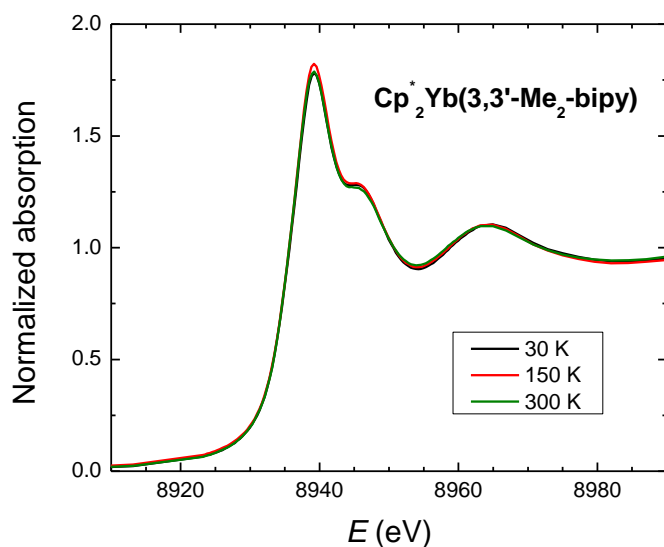


Figure 6. Yb_{LIII}-edge XANES spectra for Cp*₂Yb(3,3'-Me₂bipy) at 30 K, 150 K and 300 K. The main peak at 8939 eV is indicative of the Yb(II) contribution, and the peak at 8946 eV is indicative of the Yb(III) contribution.

Table 3. μ_{eff} and n_f values for some selected Cp'₂Yb(x,x'-bipy) adducts.

Cp'	x,x'	μ_{eff} (μ_B)	n_f (300 K)	Ref
C ₅ Me ₅	3,3'-Me ₂	0.8	0.17(2)	This work
C ₅ Me ₅	4,4'-(OMe) ₂	1.1	0.13(9)	1,12
C ₅ H ₅	H,H	1.2	0.30(1)	1,22
C ₅ Me ₅	H,H	2.4	0.83(2)	1
C ₅ Me ₅	4,4'-CO ₂ Me	3.2	0.84(2)	1

In the first two adducts in Table 3, the metallocenes are bipy adducts of (C₅Me₅)₂Yb in which the substituents on the bipyridines are methyl groups in the 3,3'-position and methoxy groups in the 4,4'-position. These two groups are electron-donating since the reduction potential of the corresponding free ligands are more negative than that in free bipy and therefore more

difficult to reduce (Table 1). Unfortunately the reduction potential for 3,3'-bipy is not available, but the influence of substituent effects is clear (see Table 1). The third and fourth adducts listed in Table 3 show the influence of the substituents on the metallocene: C₅Me₅ is more strongly reducing than C₅H₄Me, as shown in Table 1, and presumably C₅H₅, consistent with the relative value of n_f, and therefore the intermediate valence of ytterbium can be influenced by the redox potentials of the individual fragments in the adducts. This element of control was advanced in earlier work^{1,3} and the new adduct described here provides additional support for and extend this postulate to a geometrical dependence of the bipyridine ligands.

Calculations.

The CASSCF methodology, similar to the methods used in the previous studies, gives the calculated singlet-triplet energy separations and n_f values listed in Table 4.

Table 4. CASSCF Calculation results.

	S-T gap (eV)	n _f (calc)	n _f (exp)
(C ₅ H ₅) ₂ Yb(bipy)	-0.6	0.32	0.30
(C ₅ Me ₅) ₂ Yb(bipy)	-0.28 ³	0.86 ³	0.83 ¹
(C ₅ Me ₅) ₂ Yb(3,3'-Me ₂ bipy)	-0.28	0.27	0.17
(C ₅ Me ₅) ₂ Yb(4,4'-(MeO) ₂ bipy)	-0.007	0.11	0.13

The calculational results are consistent with those obtained on related bipy adducts in that the electronic ground states are open-shell singlet states that are multiconfigurational. Only one singlet is found below the triplet in each adduct in Table 4. The singlet state is composed of two configurations $f^{13}(\pi_1^*)^1$ and $f^{14}(\pi_1^*)^0$; the $f^{12}(\pi_1^*)^2$ configuration is less than 2 %. The calculated values of n_f agree with the experimental values very well for (C₅H₅)₂Yb(bipy) and (C₅Me₅)₂Yb(4,4'-(OMe)₂bipy) but the agreement is less good for the 3,3'-Me₂bipy adduct. In each case, the dominant configuration is f^{14} , in contrast to the results for (C₅Me₅)₂Yb(bipy).

Discussion.

The original reason for preparing the 3,3'-Me₂bipy adduct of Cp*₂Yb was to determine the role of the torsion angle of the bipyridine ligand on the intermediate valence of ytterbium in the resulting adduct. The NCCN torsion angle in the x,x'-Me₂bipy adducts of Cp*₂Yb are small; the torsion angle is 1° and 4° for 4,4'-Me₂bipy and 5,5'-Me₂bipy adducts, respectively, and the 2-pyridyl rings are nearly coplanar.^{3,12} When the methyl groups are in the 3,3'-position of the 2-pyridyl rings, the rings are forced out of planarity. The twisted geometry raises the energy of the LUMO, π_1^* , and presumably the reduction potential of the free ligand (see Table 1), which in turn affects the configuration of the open-shell singlet ground state and ultimately the magnetism of the adduct. This expectation is met in Cp*₂Yb(3,3'-Me₂bipy) since the torsion angle is 38°, the magnetic moment is one of the lowest observed at 300 K, as is the n_f value of 0.17. These experimental results are in reasonable agreement with the calculated value of n_f in Table 4 and the dominant configuration of the open-shell singlet ground state is $f^{14}(\pi_1^*)$.

The connection between n_f and the redox properties of the ytterbocene and the bipyridine ligand can be extended to Cp*₂Yb(4,4'-(MeO)₂bipy) and Cp₂Yb(bipy), two adducts whose low values of n_f are 0.13 and 0.30, respectively, which are independent of temperature. A methoxy group is a better electron donor than a methyl group, the Hammett σ_p values are -0.27 and -0.17, respectively²⁹ and the reduction potential of 4,4'-(EtO)₂-bipy is 0.20 V more negative than that of 4,4'-Me₂bipy (Table 3). The n_f for Cp*₂Yb(4,4'-(MeO)₂bipy) is 0.13 in accord with the larger reduction potential of the free ligand. The calculated value of n_f of 0.11 agrees with the experimental value. The reduction potential of (C₅Me₅)₂Yb⁺ is more negative than that of (C₅H₄Me)₂Yb⁺ by 0.13 V (Table 1); the value for (C₅H₅)₂Yb⁺ is not available but is likely to be slightly lower. The n_f values of the adducts of (C₅Me₅)₂Yb and (C₅H₅)₂Yb with

bipy are 0.83 and 0.30, respectively, consistent with the proposition advanced above. The calculated values of n_f of 0.86 and 0.32 agrees with experiment and these values show that the dominant configuration in the multiconfigurational ground state are inverted by changing the number of methyl substituents on the cyclopentadienyl rings.

The relation between the redox potential and n_f provides a guide to the extent of unpaired spin density located in the bipy and related heterocyclic amine adducts of ytterbocenes. The redox properties of the uncoordinated fragments in the molecular adducts, however, are only a guide since these values change on coordination; the redox potentials in Table 1 show that Cp^*_2Yb is thermodynamically incapable of reducing bipy, but electron transfer does occur. Distribution of unpaired spin density in the ligand orbitals, after the initial electron transfer event, alters the configurations involved in the multiconfigurational ground state and therefore the magnetic properties of the adducts. The amount of unpaired spin density at a given site in the ligand orbitals is crucial for understanding chemical reactivity, which is our ultimate goal. One such example, cleavage of a specific C-H bond in the 4,5-diazafluorene adduct of Cp^*_2Yb , has been published³⁰ and other will be published in due course.

Conclusions. The experimental and computational studies outlined in this and previous articles^{1,3} on the adducts formed between various ytterbocenes and substituted bipyridine ligands develops a model that accounts for their unusual magnetic properties. The experimental facts are that the ytterbium adducts are intermediate valent molecular compounds; that is, the valence of ytterbium is neither Yb(II), f^{14} , nor Yb(III), f^{13} but lies between these two extreme values. The electronic ground state is comprised of two configurations, $f^{14}(\pi_1^*)^0$ and $f^{13}(\pi_1^*)^1$, resulting in an open-shell singlet ground state that lies below the triplet state. The relative population of these two configurations, expressed as n_f , depends on the redox properties of the individual fragments of the adducts. Accordingly, the

substituents on each fragment play a role in determining the composition of the multiconfigurational ground state and ultimately the magnetic properties of the resulting adducts.³¹ The multiconfigurational ground state is, in this model, the way ytterbium avoids the extreme values of its possible oxidation numbers which allows the adducts to obey Pauling's electroneutrality principle, and behave as if they are covalent molecules.³¹⁻³³

Experimental.

General considerations. All reactions were performed using standard Schlenk-line techniques or in a drybox (MBraun). All glassware was dried at 150 °C for at least 12 h prior to use. Toluene and pentane were dried over sodium and distilled while CH₂Cl₂ was purified by passage through a column of activated alumina. Toluene-d₈ and C₆D₆ were dried over sodium. All the solvents were degassed prior to use. Infrared samples were prepared as Nujol mulls and taken between KBr plates and recorded on a Thermo Scientific Nicolet IS10 spectrometer. Samples for ultraviolet, visible, and near-infrared spectrometry were prepared in a Schlenk-adapted quartz cuvette and spectra were obtained using a Varian Cary 50 scanning spectrophotometer. Melting points were determined in sealed capillaries prepared under nitrogen and are uncorrected. Elemental analyses and mass spectra (EI) were determined by the Microanalytical Laboratory of the College of Chemistry, University of California, Berkeley. X-ray structural determinations were performed at CHEXRAY, University of California, Berkeley. Magnetic susceptibility measurements were made for all samples at 5 and 40 kOe in a 7 T Quantum Design Magnetic Properties Measurement System, that utilized a superconducting quantum interference device (SQUID). Sample containment and other experimental details have been described previously.²² The samples were prepared for X-ray absorption experiments as described previously and the same methods were used to protect the air-sensitive compounds from oxygen and water.¹ X-ray absorption measurements were made at the Stanford Synchrotron Radiation Lightsource on beamline 11-2. The samples

were prepared and loaded into a liquid helium-flow cryostat at the beamline as described previously.¹ Data were collected at temperatures ranging from 30 to 300 K, using a Si(220) double-crystal monochromator. Fit methods were the same as described previously.¹

Calculations. The ytterbium center was treated with a small-core relativistic pseudopotential (RECP) ([Ar] + 3d)³⁴ in combination with its adapted basis set (segmented basis set that includes up to g functions). The carbon, nitrogen, oxygen, and hydrogen atoms were treated with an all-electron double- ζ , 6-31G(d,p),³⁵ basis set. All the calculations were carried out with the Gaussian 03 suite of programs³⁶ and ORCA suite of program³⁷ either at the Density Functional Theory (DFT) level using the B3PW91³⁸ hybrid functional or at the CASSCF level; only one active space and inactive orbitals were used in the calculation. The geometry optimizations were performed without any symmetry constraints at either the DFT or the CASSCF level. The electrons were distributed over four 4f orbitals and the two π^* orbitals of bipyridine. The CASSCF calculations were done using the SCF orbitals. The subsequent analysis of the mixture of configuration was achieved by projecting the wavefunction on the initial orbitals, namely the SCF orbitals. This ensures that no mixing between f and π^* is present in the starting set of orbitals.

Ligand. The original synthesis of 3,3'-Me₂bipy, 3,3'-dimethyl-2,2'-bipyridine described in the literature, used the Ullmann methodology to couple two 2-bromo-3-methylpyridine molecules.³⁹ The bipyridine was reported as a viscous liquid, b.p. 293-298 °C (1 atm). A slight modification was later reported⁴⁰ and the ligand was reported as a colorless liquid whose UV spectrum agreed with the literature values.⁴¹ A ¹H NMR spectrum in Me₂CO-d₆ was reported somewhat later.⁴² The ligand used in the work reported here was purchased from SYNTHON Chemical (ChemiePark Bitterfeld Wolfen Area A, Werkstattstrasse 10, 06 766 Wolfen, Germany) as a white crystalline solid that sublimed at 90 – 100 °C onto a water cooled cold-finger under dynamic vacuum (~10⁻² mm). ¹H NMR: (C₆D₆, 293 K, δ (ppm)) 8.45 (d, J_{5,6} = 4

Hz, 2H, 6-H), 7.08 (d, $J_{4,5} = 8$ Hz, 2H, 4-H), 6.71 (dd, $J_{4,5} = 8.5$ Hz, $J_{5,6} = 5$ Hz, 2H, 5-H), 2.12 (s, 6H, Me). The ultimate proof that pure 3,3'-Me₂bipy is a solid was obtained from the X-ray crystal structures of the adducts described below.

Cp*₂Yb(3,3'-Me₂bipy). The complex Cp*₂Yb(OEt₂) (0.325 g, 0.629 mmol) was combined with 3,3'-dimethyl-2,2'-bipyridine (3,3'-Me₂bipy, 0.116 g, 0.629 mmol) and toluene (50 mL) was added at room temperature. The brown suspension was stirred at room temperature for 2 h, concentrated to ca. 25 mL and cooled to -20 °C. A dark green microcrystalline powder formed overnight (323 mg, 82%) which was recrystallized at -20 °C from warm toluene (40 °C). X-ray suitable dark green crystals formed (160 mg, 41%). The filtrate was concentrated to 15 mL and cooled at -20°C. A second and a third crop of crystals was obtained (77 mg, combined yield 70%). ¹H NMR: (toluene-d₈, 300K, δ (ppm) 32.71 (2H), 12.12 (2H, d, J= 6Hz), 8.49 (2H), 2.23 (30H, Me₅C₅), 0.58 (6H, Me). mp: 310-313°C. Anal.Calcd for C₃₂H₄₂N₂Yb: C, 61.23; H, 6.74; N, 4.46. Found: C, 61.45; H, 6.47; N, 4.32. IR (cm⁻¹): 1567 (m), 1436 (s), 1411 (m), 1380 (w), 1090 (w), 1064 (w), 1040 (w), 790(m), 741 (m), 698 (w).

[(Cp*₂Yb(3,3'-Me₂bipy)]⁺[Cp*₂YbI₂]⁻. The complex Cp*₂Yb(OEt₂) (0.204 g, 0.394 mmol) was combined in the drybox with 3,3'-Me₂bipy (0.073g, 0.394 mmol) and AgI (0.093g, 0.394 mmol). Toluene (20 mL) was added at room temperature and the brown suspension was stirred at room temperature for 16h (overnight). The resulting brown suspension was filtered and the solvent was removed under reduced pressure. The solid was triturated in pentane, the pentane was removed under reduced pressure and the residue was crystallized from warm toluene. The crystals were recrystallized twice from warm toluene (185 mg, 36%). Toluene in a ratio 1:0.33 was found in the ¹H NMR spectrum and elemental analysis. ¹H NMR: (CD₂Cl₂, 300K), δ (ppm) 331.3 (2H), 58.51 (2H), 9.84 (2H), 7.28-7.17 (m, 1.7 H, toluene), 4.17 (30H, Me₅C₅), 3.78 (30H, C₅Me₅), 2.10 (s, 1H, Toluene), -17.81 (6H, Me). ¹H NMR: (Toluene-d₈,

300K), δ (ppm) 58.46 (2H), 10.38 (2H), 6.98 (30H, Me₅C₅), 4.31 (30H, C₅Me₅), -17.59 (6H, Me). The downfield resonance due to 2H was not found in toluene. mp: >330°C. Anal. Calcd for C_{54.33}H_{74.67}N₂I₂Yb₂ (2·0.33Tol): C, 48.13; H, 5.55; N, 2.07. Found: C, 48.17; H, 5.36; N, 2.14. IR (cm⁻¹): 1604 (m), 1580 (m), 1437 (s), 1378 (m), 1188 (w), 1130 (w), 1113 (w), 1027 (w), 794 (w), 720 (m), 695 (w).

[(Cp*₂Yb(3,3'-Me₂bipy))][Cp*₂YbCl_{1.6}I_{0.4}]·CH₂Cl₂. When the product of the reaction was recrystallized by layering pentane on the top of CH₂Cl₂, instead of toluene, suitable X-ray crystals were obtained in better yield (75%), however, some of the iodide atoms were replaced by chlorine atoms. In the X-ray experiment, the compound was found to co-crystallize with CH₂Cl₂ giving the empirical formula: [(Cp*₂Yb(3,3'-Me₂bipy))][Cp*₂YbCl_{1.6}I_{0.4}]·CH₂Cl₂. The combustion analysis fits a slightly different formula: [(Cp*₂Yb(3,3'-Me₂bipy))][Cp*₂YbCl_{1.5}I_{0.5}]·CH₂Cl₂. Anal. Calcd for C₅₃H₇₄N₂I_{0.5}Cl_{3.5}Yb₂: C, 50.01; H, 5.86; N, 2.20. Found: C, 49.72; H, 5.52; N, 2.26. IR (cm⁻¹): 2850 (s), 2713 (w), 1582 (m), 1573 (m), 1439 (s), 1406 (m), 1378 (s), 1280 (m), 1237 (w), 1191(w), 1182 (w), 1167 (w), 1019 (s), 992 (w), 851 (m), 796 (s), 731 (s), 708 (m), 700 (m), 616 (w), 593 (w).

X-ray Crystallography.

Single crystals of the compounds $\text{Cp}^*_2\text{Yb}(3,3'\text{-Me}_2\text{bipy})$ and $[(\text{Cp}^*_2\text{Yb}(3,3'\text{-Me}_2\text{bipy}))][\text{Cp}^*_2\text{YbCl}_{1.6}\text{I}_{0.4}]\cdot\text{CH}_2\text{Cl}_2$ were coated in Paratone-N oil and mounted on a Kaptan loop. The loop was transferred to either a Bruker SMART 1000,⁴³ and a SMART APEX diffractometer for $\text{Cp}^*_2\text{Yb}(3,3'\text{-Me}_2\text{bipy})$ and $[(\text{Cp}^*_2\text{Yb}(3,3'\text{-Me}_2\text{bipy}))][\text{Cp}^*_2\text{YbCl}_{1.6}\text{I}_{0.4}]\cdot\text{CH}_2\text{Cl}_2$, respectively, equipped with a CCD area detector.⁴⁴ Preliminary orientation matrices and cell constants were determined by collection of 10s frames, followed by spot integration and least-squares refinement. Data were intergrated by the program SAINT⁴⁵ to a maximum 2θ value of 50.68° for $\text{Cp}^*_2\text{Yb}(3,3'\text{-Me}_2\text{bipy})$ and 50.96° for $[(\text{Cp}^*_2\text{Yb}(3,3'\text{-Me}_2\text{bipy}))][\text{Cp}^*_2\text{YbCl}_{1.6}\text{I}_{0.4}]\cdot\text{CH}_2\text{Cl}_2$. The data were corrected for Lorentz and polarization effects. Data were analyzed for agreement and possible absorption using XPREP. A semi-empirical multi-scan absorption correction was applied using SADABS.⁴⁶ This models the absorption surface using a spherical harmonic series based on differences between equivalent reflections. The structures were solved by direct methods using SHELX⁴⁷ and the WinGX program.⁴⁸ Non-hydrogen atoms were refined anisotropically and hydrogen atoms were placed in calculated positions and not refined.

Table 6. Selected crystal data for $\text{Cp}^*_2\text{Yb}(3,3'\text{-Me}_2\text{bipy})$ and $[(\text{Cp}^*_2\text{Yb}(3,3'\text{-Me}_2\text{bipy}))][\text{Cp}^*_2\text{YbCl}_{1.6}\text{I}_{0.4}]\cdot\text{CH}_2\text{Cl}_2$.

	$\text{Cp}^*_2\text{Yb}(3,3'\text{-Me}_2\text{bipy})$	$[(\text{Cp}^*_2\text{Yb}(3,3'\text{-Me}_2\text{bipy}))][\text{Cp}^*_2\text{YbCl}_{1.6}\text{I}_{0.4}]\cdot\text{CH}_2\text{Cl}_2$
Formula	$\text{C}_{32}\text{H}_{42}\text{N}_2\text{Yb}$	$\text{C}_{53}\text{H}_{74}\text{N}_2\text{Cl}_{3.6}\text{I}_{0.4}\text{Yb}_2$
Crystal size (mm)	0.3 x 0.25 x 0.10	0.45 x 0.37 x 0.15
cryst system	Orthorhombic	Triclinic
space group	<i>Pbca</i>	P-1
volume (\AA^3)	5827(3)	2582.8(6)
<i>a</i> (\AA)	17.550(5)	9.4957(14)
<i>b</i> (\AA)	18.129(5)	17.024(2)
<i>c</i> (\AA)	18.314(5)	17.198(3)
α (deg)	90	72.940(2)
β (deg)	90	76.451(2)
γ (deg)	90	87.439(2)
Z	8	2
formula weight (g/mol)	627.72	1263.65
density (calcd) (g cm^{-3})	1.431	1.749
absorption coefficient (mm^{-1})	3.247	4.060
F(000)	3024	1322
temp (K)	153(2)	110(2)
diffractometer	SMART APEX	SMART 1000
θ range for data collection (deg)	1.96 to 25.34	2.44 to 25.48
transmission range	0.393 to 0.723	0.132 to 0.481
absorption correction	Multi scan	Multi-scan
total no. reflections	49048	41199
unique reflections [R_{int}]	5319 [0.0455]	9410 [0.0264]
final R^b indices [$I > 2\sigma(I)$]	$R = 0.0247$, $R_w = 0.0522$	$R = 0.0280$, $R_w = 0.0684$
R indices (all data)	$R = 0.0354$, $R_w = 0.0574$	$R = 0.0328$, $R_w = 0.0706$
largest diff. peak and hole ($\text{e}\cdot\text{\AA}^{-3}$)	1.518 and -0.732	1.521 and -0.901
goF	1.078	1.047

ASSOCIATED CONTENT

Supporting Information. Information concerning magnetic susceptibility, Vis-NIR spectroscopy, ^1H Variable Temperature NMR, X-ray crystallography; crystal data and CIF, CCDC 943122, $\text{Cp}^*_2\text{Yb}(3,3'\text{-Me}_2\text{bipy})$, and CCDC 943123, $[(\text{Cp}^*_2\text{Yb}(3,3'\text{-Me}_2\text{bipy}))][\text{Cp}^*_2\text{YbCl}_{1.6}\text{I}_{0.4}]\cdot\text{CH}_2\text{Cl}_2$, and calculated Cartesian coordinates for $\text{Cp}_2\text{Yb}(\text{bipy})$, $\text{Cp}^*_2\text{Yb}(3,3'\text{-Me}_2\text{bipy})$ and $\text{Cp}^*_2\text{Yb}(4,4'\text{-(OMe)}_2\text{bipy})$.

AUTHOR INFORMATION

* **Corresponding Author:**

raandersen@lbl.gov(R.A.A)

ACKNOWLEDGMENT

Work at University of California, Berkeley and at Lawrence Berkeley National Laboratory was supported by the Director, Office of Energy Research, Office of Basic Energy Sciences, Chemical Sciences Division, of the U.S. Department of Energy under Contract No. DE-AC02-05CH11231. X-ray absorption data were collected at the Stanford Synchrotron Radiation Lightsource, a Directorate of SLAC National Accelerator Laboratory and an Office of Science User Facility operated for the U.S. Department of Energy Office of Science by Stanford University. We thank Wayne Lukens for several discussions on the Hubbard molecular model and Antonio DiPasquale at CHEXRAY Berkeley for his help with crystal structures.

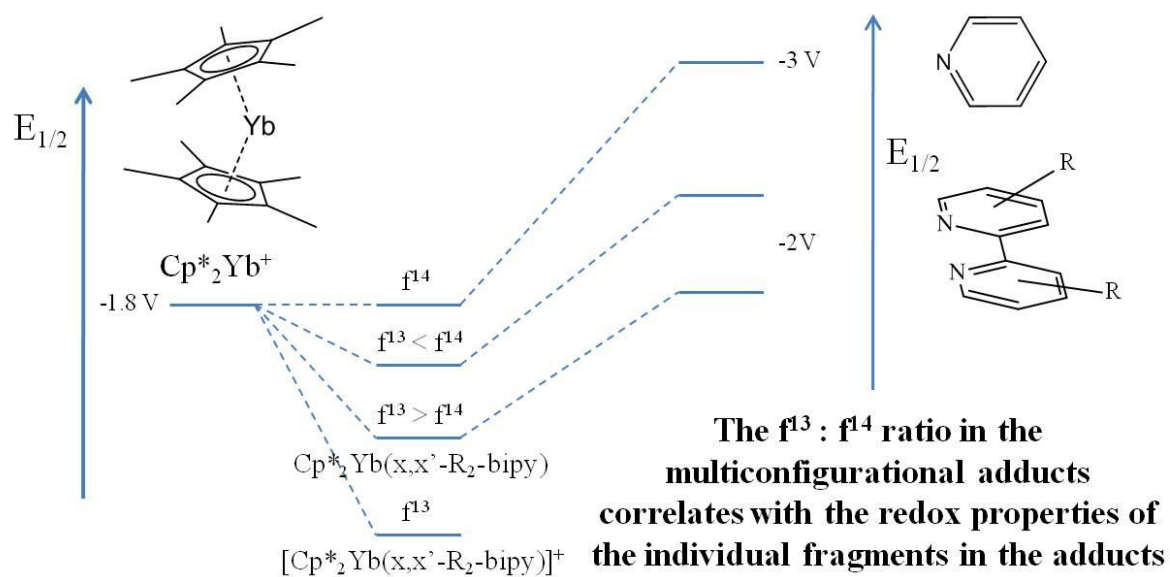
REFERENCES

- (1) Booth, C. H.; Walter, M. D.; Kazhdan, D.; Hu, Y.-J.; Lukens, W. W.; Bauer, E. D.; Maron, L.; Eisenstein, O.; Andersen, R. A. *J. Am. Chem. Soc.* **2009**, *131*, 6480.
- (2) Neumann, C. S.; Fulde, P. Z. *Phys. B Con. Mat.* **1989**, *74*, 277.
- (3) Booth, C. H.; Kazhdan, D.; Werkema, E. L.; Walter, M. D.; Lukens, W. W.; Bauer, E. D.; Hu, Y.-J.; Maron, L.; Eisenstein, O.; Head-Gordon, M.; Andersen, R. A. *J. Am. Chem. Soc.* **2010**, *132*, 17537.
- (4) Bordon, W. T. *Effects of Electron Repulsion in Diradicals* New York, 1982.
- (5) Tabner, B. J.; Yandle, J. R. *J. Chem. Soc. A* **1968**, 381.
- (6) McInnes, E. J. L.; Farley, R. D.; Rowlands, C. C.; Welch, A. J.; Rovatti, L.; Yellowlees, L. J. *J. Chem. Soc., Dalton Trans.* **1999**, 4203.
- (7) Klein, A.; Kaim, W.; Waldhor, E.; Hausen, H. D. *J. Chem. Soc., Perkin Trans.* **21995**, 2121.
- (8) Finke, R. G.; Keenan, S. R.; Schiraldi, D. A.; Watson, P. L. *Organometallics* **1986**, *5*, 598.
- (9) Watson, P. L.; Tulip, T. H.; Williams, I. *Organometallics* **1990**, *9*, 1999.
- (10) Tilley, T. D.; Boncella, J. M.; Berg, D. J.; Burns, C. J.; Andersen, R. A. *Inorg. Synth.* **1990**, *27*, 146.
- (11) Schultz, M.; Boncella, J. M.; Berg, D. J.; Tilley, T. D.; Andersen, R. A. *Organometallics* **2002**, *21*, 460.
- (12) Walter, M. D.; Berg, D. J.; Andersen, R. A. *Organometallics* **2006**, *25*, 3228.

- (13) Tilley, T. D.; Andersen, R. A.; Spencer, B.; Zalkin, A. *Inorg. Chem.***1982**, *21*, 2647.
- (14) Ohba, S.; Sato, S.; Saito, Y. *Acta Cryst. B***1979**, *35*, 957.
- (15) Ohba, S.; Miyamae, H.; Sato, S.; Saito, Y. *Acta Cryst. B***1979**, *35*, 1470.
- (16) Baxter, P. N. W.; Connor, J. A.; Wallis, J. D.; Povey, D. C.; Powell, A. K. *Polyhedron***1992**, *11*, 1771.
- (17) Cheng, W.-C.; Yu, W.-Y.; Zhu, J.; Cheung, K.-K.; Peng, S.-M.; Poon, C.-K.; Che, C.-M. *Inorg. Chim. Acta***1996**, *242*, 105.
- (18) Craig, D.; Goodwin, H.; Onggo, D. *Aust. J. Chem.***1988**, *41*, 1157.
- (19) Varela, J. A.; Castedo, L.; Maestro, M.; Mahía, J.; Saá, C. *Chem. Eur. J.***2001**, *7*, 5203.
- (20) Sato, S.; Saito, Y. *Acta Cryst. B***1978**, *34*, 3352.
- (21) The H-3 and H-5 resonances in ref (12) are incorrectly assigned; the correct assignment is in ref (3).
- (22) Walter, M. D.; Schultz, M.; Andersen, R. A. *New J. Chem.***2006**, *30*, 238.
- (23) Banci, L.; Bertini, I.; Luchinat, C.; Pierattelli, R.; Shokhirev, N. V.; Walker, F. A. *J. Am. Chem. Soc.* **1998**, *120*, 8472.
- (24) Oki, M. In *Topics in Stereochemistry* 1983; Vol. 14, p 1.
- (25) Ashby, M. T.; Alguindigue, S. S.; Schwane, J. D.; Daniel, T. A. *Inorg. Chem.* **2001**, *40*, 6643.
- (26) Ashby, M. T. *J. Am. Chem. Soc.***1995**, *117*, 2000.
- (27) Ashby, M. T.; Alguindigue, S. S.; Khan, M. A. *Organometallics***2000**, *19*, 547.
- (28) Da Re, R. E.; Kuehl, C. J.; Brown, M. G.; Rocha, R. C.; Bauer, E. D.; John, K. D.; Morris, D. E.; Shreve, A. P.; Sarrao, J. L. *Inorg. Chem.***2003**, *42*, 5551.
- (29) Streitwieser, A.; Heathcock, C. H.; Kosower, E. M. *Introduction to Organic Chemistry*; Mcmillan Publishing Compagny: New York, 1992.
- (30) Nocton, G.; Booth, C. H.; Maron, L.; Andersen, R. A. *Organometallics***2013**, *32*, 1150.
- (31) Lukens, W. W.; Magnani, N.; Booth, C. H. *Inorg. Chem.***2012**, *51*, 10105.
- (32) Denning, R. G.; Harmer, J.; Green, J. C.; Irwin, M. *J. Am. Chem. Soc.***2011**, *133*, 20644.
- (33) Neidig, M.L., Clark, D.L., Martin, R.L. *Coord.Chem.Rev.* **2013**, *257*, 394
- (34) Dolg, M.; Stoll, H.; Preuss, H. *J. Chem. Phys.***1989**, *90*, 1730.
- (35) Harihara.Pc; Pople, J. A. *Theor. Chim. Acta***1973**, *28*, 213.
- (36) Frisch, J.; Revision E-01 ed.; Gaussian Inc.: Pittsburgh, PA, 2001.
- (37) Neese, F.; Version 2.4. ed.; Chemie, M.-P.-I. f. B., Ed. Mülheim and der Ruhr, 2004.
- (38) Becke, A. D. *J. Chem. Phys.***1993**, *98*, 5648.
- (39) Case, F. H. *J. Am. Chem. Soc.***1946**, *68*, 2574.
- (40) Nakamaru, K. *Bull. Chem. Soc. Jpn.***1982**, *55*, 2697.
- (41) Suzuki, T. M.; Kimura, T. *Bull. Chem. Soc. Jpn.***1977**, *50*, 391.
- (42) Rebek, J.; Trend, J. E.; Wattley, R. V.; Chakravorti, S. *J. Am. Chem. Soc.***1979**, *101*, 4333.
- (43) Bruker Analytical X-Ray System, I. Madison, Winsconsin, USA, 2007.
- (44) Bruker Analytical X-Ray System, I. Madison, Winsconsin, USA, 2007.
- (45) Bruker Analytical X-Ray System, I. Madison, Winsconsin, USA, 2007.
- (46) Blessing, R. *Acta Cryst. A***1995**, *51*, 33.

- (47) Sheldrick, G. *Acta Cryst. A* **2008**, *64*, 112.
 (48) Farrugia, L. *J. Appl. Cryst.* **1999**, *32*, 837.

Table of Content



DISCLAIMER

This document was prepared as an account of work sponsored by the United States Government. While this document is believed to contain correct information, neither the United States Government nor any agency thereof, nor the Regents of the University of California, nor any of their employees, makes any warranty, express or implied, or assumes any legal responsibility for the accuracy, completeness, or usefulness of any information, apparatus, product, or process disclosed, or represents that its use would not infringe privately owned rights. Reference herein to any specific commercial product, process, or service by its trade name, trademark, manufacturer, or otherwise, does not necessarily constitute or imply its endorsement, recommendation, or favoring by the United States Government or any agency thereof, or the Regents of the University of California. The views and opinions of authors expressed herein do not necessarily state or reflect those of the United States Government or any agency thereof or the Regents of the University of California.